OPTICAL AND SPECTROSCOPIC PROPERTIES OF Er^{3+}DOPED $60Sb_2O_3$-$10Na_2O$-30PbO GLASS

MANSOURA MANCER, MOHAMED TOUFIK SOLTANI

Laboratoire de Physique Photonique et nanomatériaux multifonctionnels, Université de Biskra, BP 145, Biskra, Algérie

mnsrmnsr43@gmail.com

ABSTRACT

Er^{3+}doped sodium lead antimonite glass have been prepared and analyzed by (UV-Vis-NIR) absorption, near infrared luminescence and fluorescence decays. The optical band gap and refractive index were calculated from the (UV-Vis-NIR) absorption. The Judd-Ofelt theory has been applied to compute the J–O intensity parameters Ωt (t= 2, 4, 6) from absorption spectrum and determine the spectroscopic parameters such as the radiative transition probability (A_{rad}), radiation lifetime (τ) and branching ratio (β) of Er^{3+} transition. Experimental lifetime of the glass for the transition between $^4I_{13/2}$ and $^4I_{15/2}$ level was calculated from the photoluminescence decay curves and estimated the quantum efficiency. Absorption, emission and gain cross-section, effective band width ($\Delta\lambda_{eff}$) and gain band width of the $^4I_{13/2} \rightarrow {}^4I_{15/2}$ transition of Er^{3+} in glass are recorded and calculated. The obtained results confirm the potential of this glass in signal amplification and laser application.

KEYWORDS: Spectroscopic properties, Antimony oxide glass, Er doping, Judd–Ofelt theory, Band gap, emission cross-section.,

1 INTRODUCTION

Er^{3+} doped glasses are very important because of the possibility of their application in optoelectronic and optic device fields, such as lasers, fiber optic and solar cells [1.2]. For higher efficiency must choose host material glasses which are characterized low Phonon energies. Heavy-metal oxide glasses (HMO) have studied been widely as host materials for Er3+ ion in recent years because they possess low Phonon energies [2]. Among them, Sb2O3-based glasses possess easier preparation, large transparency window, low phonon energy (605 cm_1), better thermal stability, high refractive index (n=2), and better chemical durability than that of fluoride or tellurite glasses [3.4.5]. There are several studies on Er^{3+} doped sodium antimony glasses containing ZnO, WO_3 or Bi_2O_3. In the present study sodium antimony lead glass (Sb_2O3–Na_2O–PbO) is used as the glass host for Er^{3+} ions and this paper describe The (UV-V) absorption spectrum of the glass has been measured and the optical band gap and refractive index have been determined. From optical absorption were computed the experimental oscillator strengths of the transitions from the ground state to the excited levels and using Judd–Ofelt theory to calculate the intensity parameters Ωt (t = 2, 4, 6), radiative transition probability, branching ratios, radiative lifetimes and computed absorption cross-section (σ_a).The stimulated emission cross-section (σ_e) and gain cross-section (σ_g) of $^4I_{13/2} \rightarrow {}^4I_{15/2}$ transition at around 1.53 μm are obtained based on the Füchtbauer–Ladenburg equation and Photoluminescence spectra measurement.

2 EXPERIMENTAL PROCEDURE

60Sb2O3-10Na2O-30PbO glass doped with 0.25% Er2O3 was prepared by the conventional melt-quenching method.

the optical, spectroscopic and luminescent properties obtained for $60Sb_2O_3$-$10Na_2O$-30PbO doped with 0.25(mol.%) Er^{3+}.

The synthesis was carried out through the conventional melt-quenching method from starting commercial powders of Sb2O3 (99+%), ACROS ORGANICS, sodium carbonate (99.8 min), PbO (99% Alfa Aesar), and Er2O3 (99.9% Sigma Aldrich) are used as raw materials. The obtained glass is denoted SN3PE. For preparation of sample follow the following steps firstly, weighing and mixing of the powders (5g) and placed in a silica tube. Secondly, the tube is heated during 5 to 10 min on heat flame at a temperature close to 850 °C and the tube was shaken until we observed a homogeneous liquid. The liquid is poured onto a brass plate at 250 °C. The end step is annealing at 300°C and slow cooling down to room temperature and polished for optical measurements. The density was obtained by Archimedes principle using distilled water as medium. The absorption spectra of the sample were measured in the 300–3000 nm interval using a UV–Vis–NIR spectrophotometer (Perkin– Elmer Lambda 900). The emission spectra were recorded in a Horiba Yvon spectrofluorometer Fluorolog using a xenon lamp (450w).Time correlated single photon counting (TCSPC) resolved fluorescence data were collected on a TCSPC Fluorolog using a Xenon flash lamp (450w). The fluorescence decay was recorded using pulsed laser excitation at 980 nm. All the optical measurements

were performed at room temperature.

3 RESULTS AND DISCUSSION

3.1 Density and Optical properties

The measured density of Er^{3+} doped SN3P glass sample is ρ=5.45(g/cm^3)and the concentration of Er^{3+} ions is 6.61 (10^{19} ions cm^{-3}). The refractive index value for sample is used in this work is calculated by using the equation following [8]

$$\frac{n^2-1}{n^2+1}=1-\sqrt{\frac{E_{opt}}{20}} \quad (1)$$

Where E_{opt} is the optical band gap of the glass, which is calculated from optical absorption edges using Tauc model. This value of refractive index is 2.077.

3.2 Absorption spectrum and Judd–Ofelt analysis

Figure 1 represents the optical absorption spectrum of the sample glass in the range of 350_1700 nm at room temperature. The absorption cross-section spectra $\sigma_\alpha(\lambda)$ were calculated from the relation:

$$\sigma_\alpha(\lambda)=\frac{\alpha(\lambda)}{N} \quad (2)$$

Where N is the E3+ doping concentration and $\alpha(\lambda)$ is the absorption coefficient [9].The absorption coefficient spectra of sample consist of seven sharp peak at 1530,974,799,652, 544,522,489 nm corresponding to the transition from ground stat $^4I_{15/2}$ to the excited stats $^4I_{13/2}$, $^4I_{11/2}$, $^4I_{9/2}$, $^4F_{9/2}$, $^4S_{3/2}$, $^2H_{11/2}$, $^4F_{7/2}$ and these transition are labeled in the Fig.1.

Judd-Ofelt theory is widely used to analyze absorption coefficient spectra. From radiative transition and using Judd-Ofelt theory can be determined of the J–O intensity parameters Ω2, Ω4 and Ω6 (Ωt ,t= 2, 4, 6), the spontaneous emission probabilities (A_R), the branching ratios (B) and the radiative lifetime (τ).The experimental oscillator strength f_{exp} for the transition from the ground $^4I_{15/2}$ (J = 15/2) manifold to the excited J' manifolds can be calculated from the absorption spectrum using the formula:

$$F_{\exp}=\frac{mc^2}{\pi e^2\lambda_{abs}^2 N}\Gamma \quad (3)$$

Where m and e are the electron mass and charge, respectively, c is the velocity of light, N is the concentration of Er^{3+} in the glass , which are listed in Table 1 and λ_{abs} is the mean wavelength of the absorption band and Γ is the integrated absorption coefficient[10]. The calculated electric-dipole transition oscillator strength $F_{ed}^{\exp}$ is expressed as:

$$F_{ed}^{\exp}=F_{\exp}-F_{md} \quad (4)$$

Where F_{md} is the magnetic -dipole transition oscillator strength and is defined as:

$$F_{md}=\frac{8\pi^2 mc}{3h(2j+1)\lambda}\cdot X_{md}\cdot S_{md} \quad (5)$$

Where h is the Planck constant, X_{md}=n and n is refractive index and S_{md} are the magnetic dipole line strength of an electronic transition from an initial (S, L) J state to the final $(S',L')J'$ is defined as:

$$S_{md}=\left(\frac{h}{4\pi mc}\right)^2\left(\langle[L,S]J\,||L+2S||\,[L',S']J'\rangle\right)^2 \quad (6)$$

where (L + 2S) is the md operator and in this work, the values of $\langle[L,S]J\,||L+2S||\,[L',S']J'\rangle$ was calculated by relations in ref [11]. The experimental and calculated electronic dipole line strength of an electronic transition from an initial (S, L) J state to the final $(S',L')J'$ can be calculated from equations (7) and (8) respectively:

$$S_{ed}^{\exp}=(3h(2J+1)\lambda F_{ed}^{\exp})/(8\pi^2 mcX_{ed}) \quad (7)$$

$$S_{ed}^{cal}=\sum\Omega_t\left(\langle[L,S]J\,||U^t||\,[L',S']J'\rangle\right)^2 \quad (8)$$

Where $X_{ed}=(n^2+2)^2/9n$, U^t are the doubly reduced matrix elements of rank (t=2,4 and 6) and The values of the doubly reduced matrix elements of rank were used in this work we were taken from [12] [13]. Thus The J–O intensity parameters Ωt (t = 2, 4, 6) can be derived from the experimental and calculated electronic dipole line strength of an electronic. The root mean-square deviation (RMS) is

determined by:

$$RMS = \sqrt{\frac{1}{q-p}\sum_{i=1}^{q}\left(S_i^{\exp} - S_i^{calc}\right)^2} \qquad (9)$$

Where q is the number of transitions and p is the number of parameters determined where in this work the values of q and p are7 and 3 respectively.

Table 1 shows the values of the mean wavelength of the absorption band (λ), the integrated absorption coefficients (Γ), the experimental and calculated electronic dipole line Strength, the experimental and calculated electronic oscillator strength, the magnetic electronic dipole line strength and the magnetic electronic oscillator strength for sample glass.

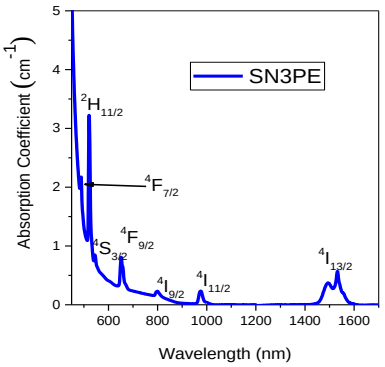

Figure 1: Room temperature absorption coefficient of 60Sb2O3–10Na2O–30PbO_0.25Er2O3 glass sample (SNP3E).

Table 01 : the values of the mean wavelength of the absorption band (λ), the integrated absorption coefficients (Γ), the experimental and calculated electronic dipole line strength and oscillator strength, the magnetic electronic dipole line strength and oscillator strength of sample glass.

Transition $^4I_{15/2}$	$\lambda(nm)$	$\Gamma(cm^{-1}\,\mathrm{nm})$	Line strength ($10^{20}cm^2$)			Oscillator strength ($10^{-6}cm^2$)		
			$S_{ed}^{\exp}$	S_{ed}^{cal}	S_{md}^{cal}	$F_{ed}^{\exp}$	F_{ed}^{cal}	F_{md}^{cal}
$^4I_{13/2}$	1532	32	1.76	1.67	0.71	1.67	1.58	0.66
$^4I_{11/2}$	976	4.40	0.53	0.51	0	0.79	0.76	0
$^4I_{9/2}$	799	2.43	0.36	0.29	0	0.65	0.52	0
$^4F_{9/2}$	652	7.42	1.34	1.31	0	2.98	2.92	0
$^4S_{3/2}$	545	0.92	0.20	0.21	0	0.53	0.57	0
$^2H_{11/2}$	521	18.18	4.10	4.10	0	11.39	11.40	0
$^4F_{7/2}$	489	2.49	0.60	0.84	0	1.78	2.50	0

Table 02: J–O intensity parameters and spectroscopic quality factor for SN3PE glass and comparison with other glasses systems.

glass host	Ω_2	Ω_4	Ω_6	RMS	Ω_4/Ω_6	References
	($10^{-20}cm^2$)					
SN3PE	4,697	1,618	0,968	0,14	1,67	present work
SNZE0.25	4.39	1.22	0.66		1.85	[6]
SWNB0.25	6.46	1.53	1.92	0.17	0.79	[7]
ZBLAN	2.91	1.78	1.00		1.78	[17]
Silicat	4.23	1.04	0.61		1.70	[18]
Phosphate	3.91	1.97	2.57		0.76	[19]
tellurite	4.76	1.06	0.89	0.17	0.83	[8]
germinate	5.43	0.52	0.38	0.10	0.73	[20]

Table 2 displays the values of The J–O intensity parameters Ωt (t = 2, 4, 6) and the root mean-square deviation (RMS) for glass sample with other glasses. From table 2 the value of Ω2 for SN3PE glass is larger than those for ZBLAN, phosphate, tellurite, SNZE0.25 and silicate glasses. The value of Ω_2 for SN3PE glass is lower than those for SWNB0.25 and germinates glasses. This indicates that Er3+ ions in the SN3P glass presents lower covalency of the ions-ligand and higher symmetry when compared with germinate and SWNB0.25glasses and higher covalency of the ions-ligand and lower symmetry when compared with ZBLAN, phosphate, SNZE0.25 and silicate glasses. While

the values of Ω_4 and Ω_6 are smaller than values of Ω_2 and may be due to the rigidity of the studied glass [14]. According to Jacobs and Weber theory, the erbium emission intensity could be characterized uniquely by Ω_4 and Ω_6 parameter. Thus, we use the so-called spectroscopic quality factor χ, defined as $\chi=(\Omega_4/\Omega_6)$. [8.15] .The smaller this factor value due to the more intense laser transition; therefore this factor is important used to measure the lasing efficiency of a material. The value of factor χ for sample is listed in Table 2 and this parameter is smaller than those for ZBLAN, SNZE0.25 and silicate glasses so this glass is good for laser application.

The total spontaneous emission probability from the excited state J' and the terminating state J is relates by the magnetic and electric dipole transitions can be calculated using the following relation [20]:

$$A(J' \to J) = A_{ed} A(J' \to J) + A_{md} A(J' \to J) \quad (10)$$

$$A(J' \to J) = \frac{(64\pi^4 e^2 n^2)}{(3h(2J'+1)\lambda^3)} (X_{ed} S_{ed} + X_{md} S_{md}) \quad (11)$$

Where S_{ed} is calculated using Eq. (8), A_{ed} and A_{md} are the electric-dipole and magnetic-dipole spontaneous emission probabilities, respectively.

The radiative lifetime τ of the excited state J is simply related to the total spontaneous emission probability $A_{J'J}$ and the branching ratio $B_{J'J}$ can be determined by[21]:

$$\tau = 1/A_{J'J} \quad \text{with} \quad A_{J'J} = \sum_{J''} A(J' \to J'') \quad (12)$$

$$B_{J'J} = \frac{A(J' \to J'')}{\sum_{J''} A(J' \to J'')} \quad (13)$$

J'' is being the intermediate states lying between J' and J.

The branching ratios and the radiative lifetime are critical parameters to the laser designer because they characterize the possibility of attaining stimulated emission from any specific transition. The spontaneous emission probabilities (A), the branching ratios (b) and the radiative lifetime (τ) of the SN3PE glass are summarized in Table 3. The value of radiative lifetime for the sample is lower than those in SNZE0.25, phosphate, ZBLAN, tellurite and sodium lead germinate glasses and larger than those in SWNB0.25 glass.

Table 03: Calculated radiative probabilities A, branching ratios B and radiative lifetimes for glass.

Transition	*State energy*	*radiative probabilities $A_r(s^{-1})$*		*β (%)*	*τ (ms)*
SLJ→ SL'J'	*(cm^{-1})*	*A_{ed}*	*A_{md}*		
$^4I_{13/2}\rightarrow{}^4I_{15/2}$	6527	221.85	92.68	100	3.180
$^4I_{11/2}\rightarrow{}^4I_{13/2}$	3600	38.64	23.99	17.43	2.780
$^4I_{11/2}\rightarrow{}^4I_{15/2}$	10100	296.59	0	82.56	
$^4I_{9/2}\rightarrow{}^4I_{11/2}$	2150	1.64	4.61	1.38	2.202
$^4I_{9/2}\rightarrow{}^4I_{13/2}$	5750	90.72	0	19.98	
$^4I_{9/2}\rightarrow{}^4I_{15/2}$	12250	357.12	0	78.64	
$^4F_{9/2}\rightarrow{}^4I_{9/2}$	2900	10.42	0	0.31	0.297
$^4F_{9/2}\rightarrow{}^4I_{11/2}$	5050	137.33	0	4.079	
$^4F_{9/2}\rightarrow{}^4I_{13/2}$	8650	158.156	0	4.69	
$^4F_{9/2}\rightarrow{}^4I_{15/2}$	15150	3060.76	0	90.91	
$^4S_{3/2}\rightarrow{}^4I_{9/2}$	6100	142.04	0	4.22	0.297
$^4S_{3/2}\rightarrow{}^4I_{11/2}$	8250	73.67	0	2.19	
$^4S_{3/2}\rightarrow{}^4I_{13/2}$	11850	933.93	0	27.76	
$^4S_{3/2}\rightarrow{}^4I_{15/2}$	18350	2214.78	0	65.83	
$^2H_{11/2}\rightarrow{}^4F_{9/2}$	4000	62.30	0	0.37	0.059
$^2H_{11/2}\rightarrow{}^4I_{9/2}$	6900	249.39	0	1.48	
$^2H_{11/2}\rightarrow{}^4I_{11/2}$	9050	176.86	0	1.05	
$^2H_{11/2}\rightarrow{}^4I_{13/2}$	12650	291.58	0	1.73	
$^2H_{11/2}\rightarrow{}^4I_{15/2}$	19150	16094.52	0	95.38	
$^4F_{7/2}\rightarrow{}^4F_{9/2}$	5150	14.51	41.49	0.70	0.125
$^4F_{7/2}\rightarrow{}^4I_{9/2}$	8050	281.78	0	3.53	
$^4F_{7/2}\rightarrow{}^4I_{11/2}$	10200	525.91	0	6.59	
$^4F_{7/2}\rightarrow{}^4I_{13/2}$	13800	1201.29	0	15.05	
$^4F_{7/2}\rightarrow{}^4I_{15/2}$	20300	5913.86	0	74.12	

3.3 Fluorescence decay and Photoluminescence at 1.5mm

Fig.2A shows the fluorescence decay curve for the $^4I_{13/2}\rightarrow{}^4I_{15/2}$ transition of Er^{3+} doped SN3P glass. By fitting the decay 1 curve the lifetime of $^4I_{13/2}$ level could be evaluated. The value of experimental lifetime is 3.13ms. Furthermore, this result is compared to those of other laser materials as shown in table 4, which is longer than those in SWNB0.25 glass but lower than those for SNZE0.25, phosphate, ZBLAN, tellurite and sodium lead germinate glasses. These radiative and experimental lifetime were used to compute the quantum efficiency of the sample glass ($\eta=\tau_{meas}/\tau$), as listed in Table 4. It can be seen from Table 4 that SN3PE glass presents high quantum efficiency than other glasses (98%). This result indicates that the proposed glass can be considered a good candidate for use in mead infrared (MIR) lasers.

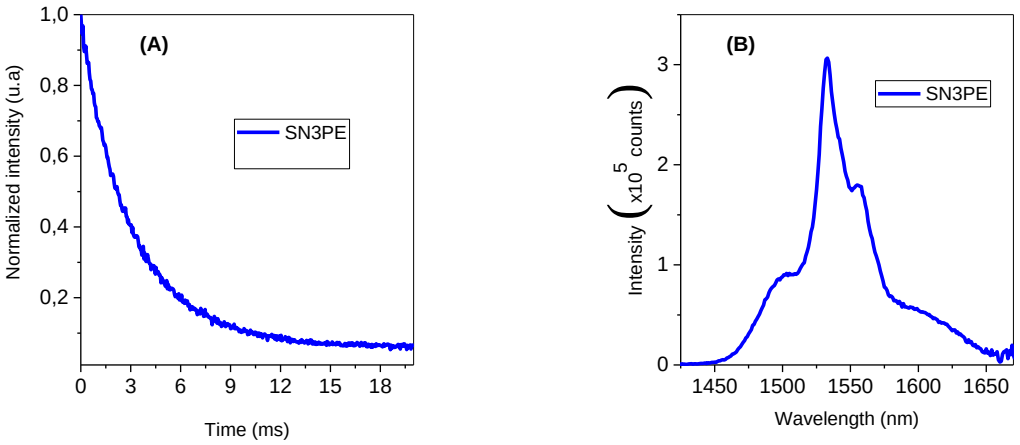

Figure 2: (A) Fluorescence decay time of 4I13/2→4I15/2 transition for Er3+ doped SN3P glass.(B) Emission spectra of SN3PE sample.

Table 04: The experimental, radiative lifetime (ms) and quantum efficiency (η %) for SN3PE glass and comparison with other glasses systems

glass host	Lifetime (ms)		Quantum efficiency (%)	reference
	Radiative	Experimental		
SN3PE	3.18	3.13	98	This work
SNZE0.25	4.91	3.35	68.22	[6]
SWNB0.25	2.94	2.67	90.81	[7]
ZBLAN	9.52	8.69	91	[17]
Phosphate	7.53	3.95	52	[19]
tellurite	4.79	3.46	72	[8]
germinate	9.70	7.62	79	[20]

The photoluminescence spectra of the strong emission band at 1532 nm of the sample glass is recorded under direct excitation of Er^{3+} ions (λ_{exc}=980 nm) at room temperature and is shown inFig.2B. The band over the range of 1400–1700 nm arises from the $^4I_{13/2}\rightarrow{}^4I_{15/2}$ transition.

The absorption cross-section spectra (σ_a), emission cross-section spectra (σ_e) and the effective band width of emission

spectra of the $^4I_{13/2}\rightarrow{}^4I_{15/2}$ transition in SN3PE glass are computed. The absorption cross section spectra can be calculated by equation (2). Based on the photoluminescence spectra, the stimulated emission cross section spectra can be determined by using the Füchtbauer–Ladenburg equation [22]

$$\sigma_e(\lambda)=\frac{\lambda^5}{8\pi cn^2\tau}\frac{I(\lambda)}{\int\lambda I(\lambda)d\lambda} \qquad (14)$$

Where λ is the emission wavelength, τ is the radiative lifetime, n is the refractive index and I(λ) is the emission spectrum intensity. The effective band width $\Delta\lambda_{eff}$ of emission spectra is defined as $\Delta\lambda_{eff}=\int I(\lambda)d\lambda / I_{max}$ where I_{max} is the emission intensity at peak emission wavelength. From The effective band width $\Delta\lambda_{eff}$. Stimulated emission cross-section spectra (σ_e) and, radiative lifetime (τ), can be calculated. Tow parameters are most important for the application of the amplifier and these parameters are the gain bandwidth ($\sigma_e\times\Delta\lambda_{eff}$) and the optical gain parameter ($\sigma_e\times\tau$).

Fig.3A shows the absorption and emission cross-section spectra for sample.

The maximum absorption, emission cross-section, effective band width, gain bandwidth (σe×Δλeff) and optical gain parameter (σe×τ) at ~1532 are listed in Table 5. The full-width at half-maximum (FWHM) was also calculated and listed in Table 6. The larger value for the emission cross-section is related to the larger value of the spontaneous radiative transition probability of the $^4I_{13/2}\rightarrow{}^4I_{15/2}$ transition. This consideration explains why the emission cross-section value in our case is larger than those in SNZE0.25, ZBLAN, Phosphate, tellurite and sodium lead germinate glasses and lower that in SWNB glass.

Table 05:The effective width $\Delta\lambda_{eff}$ (nm), FWHM (nm), absorption cross-section σ_a ($10^{-21}cm^2$), emission cross-section σ_e ($10^{-21}cm^2$), FWHM×σ_e ($10^{-21}cm^2$), optical gain $\sigma_{em}\times\tau$ ($10^{-21}cm^2$) and gain bandwidth $\sigma_e\times\Delta\lambda_{eff}$ ($10^{-21}cm^2$nm) relative to the PL band at 1.532 mm and radiative probabilities A(s^{-1})for SN3PE glass and comparison with other glasses systems

glass host	FWHM	A	$\Delta\lambda_{eff}$	σ_a	σ_e	FWHM×σ_e	$\sigma_{em}\times\tau$	$\sigma_e\times\Delta\lambda_{eff}$	reference
SN3PE	38.68	313.0	58.31	8.50	09.22	356.63	29.32	537.62	present work
SNZE0.25	36.00	203.6	55.00	6.76	07.26	261.36	35.65	399.30	[6]
SWNB0.25	55.00	340.1	64.60	6.86	10.70	588.50	31.46	691.22	[7]
ZBLAN	82.00	100.0	/	/	04.20	344.40	39.98	/	[18]
Phosphate	43.84	132.0	65.41	/	07.70	337.58	57.98	503.66	[19]
tellurite	49.32	208.0	61.86	6.33	07.93	391.00	38.12	490.00	[8]
germinate	19.00	103.5	34.60	/	07.40	140.60	71.78	256.04	[20]

The emission and absorption cross section spectra were used to calculate gain cross section spectra using following equation:

$$\sigma g(\lambda) = \beta\sigma e(\lambda)-(1-\beta)\sigma a(\lambda) \quad (15)$$

Where the population inversion βis the ratio of Er3+ concentration in the lasing state $^4I_{13/2}$ to that in the ground state$^4I_{15/2}$ and β (0 to 1 with the increases of 0.2)

[22][16]. Fig.3B shows the gain cross section spectra for SN3PE glass as a function of the population inversion β. The SNP3E glass displays for population inversion of 60%, the gain cross section Spectra is positive in the range from 1515 to 1681 nm and it is relatively flat, which is very interesting for applications of wavelength division multiplexing (WDM)[6] [23]. At (β=1) all ion are in the excited state the gain cross section is 9.22 cm2 at 1532 nm and this σg value is better than this in SNZE1 glass (7.14× 10^{-21}cm²)[6].

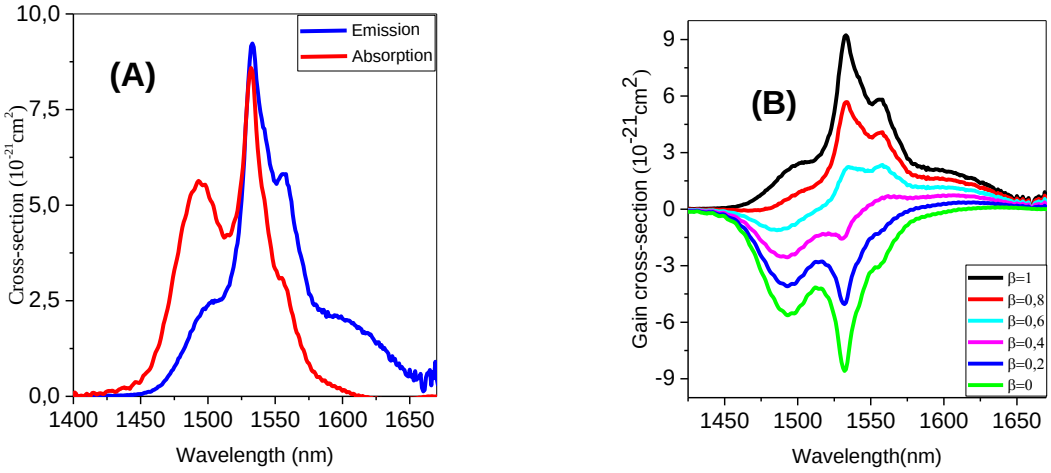

Figure 3(A): Absorption and Emission cross-section spectra of SN3PE glass.(B) Gain cross-section spectra in SN3PE glass

4 CONCLUSIONS

In this study, the effect of the lead PbO on the optical and spectroscopic properties of the Er3+ doped antimony sodium glass is investigated from the absorption spectra and the photoluminescence spectra fluorescence decay curve for the $^4I_{13/2}\rightarrow{}^4I_{15/2}$ transition. The optical band gap values indicated that this glass is amorphous semiconductors. The refractive index values are high (n≥2). The oscillator strengths, the J–O intensity parameters, the spectroscopic quality factor, the total spontaneous emission probability, the branching ratios and the radiative lifetimes were calculated based on the experimental absorption spectrum and the J–O theory. The SN3PE glass presents high quantum efficiency (η=98%), the emission cross-sections obtained from Füchtbauer–Ladenburg methods is 9.22×10^{-21}cm² at 1532 and shows higher value than in other glasses such as 7.28×10^{-21}cm² for SNZE0.50 glass. Summarizing, Er^{3+} doped the lead-sodium-antimonite glass is good glass for laser application.

REFERENCES

[1] G Lakshminarayana, Jianrong Qiu, M G Brik, G AKumar and I V Kityk, J. Phys.Condens. Matter.20 (2008) 375104 (12pp).

[2] Mi-Yeon Yoo, Jin-Ho Lee, Hong-Myeong Jeong, Ki-Soo Lim, P. Babu, J. Optical. Materials. 35 (2013) 1922–1926.

[3] M. Baazouzi, M.T. Soltani, M. Hamzaoui, M. Poulain, J. Troles, J. Optical. Materials. 36 (2013) 500–504.

[4] A.E. Ersundu, M. Celikbilek, M. Baazouzi, M.T. Soltani, J. Troles, S. Aydin, J. Alloys Comp. 615 (2014) 712–718.

[5] M. Çelikbilek Ersundua, A.E. Ersundua, M.T. Soltanib, M. Baazouzi,J. ceramint. 43 (2017) 491–497.

[6] M. Hamzaoui1, M. T. Soltani, M. Baazouzi, B. Tioua, Z. G. Ivanova, R. Lebullenger, M. Poulain1, and J. Zavadil, J. Jallcom Phys. Status Solidi. B (2012).

[7] K. Ouannes, M.T. Soltani, M. Poulain, G. Boulon, G. Alombert-Goget c, Y. Guyot c, A. Pillonnet c and K. Lebbou, J. jallcom. 603 (2014) 132–135.

[8] Hssen Fares, Habib Elhouichet, Bernard Gelloz, and Mokhtar Férid, J. Appl. Phys. 116, 123504 (2014).

[9] Chun Li, Ying Zhang, Xuejian Zhang, Dongwei Miao, Hai Lin, Mauro Tonelli, Fanming Zeng and Jinghe Liu, J. msa. 2011, 2, 1161-1165.

[10] BoWei, Zhoubin Lin, Lizhen Zhang and GuofuWang, J. Phys. D. Appl. Phys. 40 (2007) 2792–2796.

[11] A Lira C, I Camarillo, E Camarillo, FRamos, M Flores and U Caldi˜no, J. Phys. Condens. Matter 16 (2004) 5925–5936

[12] W. T. Carnall, P. R. Fields, and K. Rajnak, J. Chero. Phys. 21, 637 (1953).

[13] Dhiraj K. Sardar, John B. Gruber, Bahram Zandi, J. Andrew Hutchinson and C. Ward Trussell, J. Appl. Phys., Vol. 93, No. 4, 15 February 2003.

[14] N. Sdiri, H. Elhouichet, C. Barthou c and M. Ferid, j. molstruc. 1010 (2012) 85–90.

[15] Gokulakrishnan Soundararajan, Cyril Koughia, Andy Edgar, Chris Varoy, Safa Kasap, j .jnoncrysol. 357 (2011) 2475–2479.

[16] I. Jlassi, H.Elhouichet, M.Ferid and C.Barthou, j. jlumin. 130 (2010) 2394–2401.

[17] L. Wetenkamp 1, G.F. West and H. T6bben, J. Non-Crystalline Solids. 140 (1992) 35-40.

[18] Jianhu Yang, Shixun Dai, Yuefen Zhou, Lei Wen, Lili Hu et al. J. Appl. Phys. Vol. 93, No. 2, 15 January 2003.

[19] A. Langar, C. Bouzidi, H. Elhouichet, M. Férid.J. jlumin.2013.12.008.

[20] M. Jiménez de Castro and J.M. Fernández Navarro, J. Appl Phys B (2012) 106:669–675.

[21] Xiaodong Xu, Guangjun Zhao, Feng Wu, Wenwei Xu, Yanhua Zong, Xiaodan Wang, Zhiwei Zhao, Guoqing Zhou and Jun Xu, j. jcrysgro. 310 (2008) 156–159.

[22] Guokui Liu and Bernard Jacquier, Springer Berlin Heidelberg New York. ISBN 3-540-23886-7

[23] K. Venkata Krishnaiah, K. Upendra Kumar, V. Agarwal, C.G. Murali, S. Chaurasia, L.J. Dhareshwar, C.K. Jayasankar and Victor Lavin, j. phpro. 29 (2012) 109 – 113.

[24] Daqin Chen, Yuansheng Wang1, Yunlong Yu, En Ma and Zhongjian Hu, J. PhysCM. 17 (2005) 6545–6557.